

# Formation of New Type of Porous Carbon by Carbonization in Zeolite Nanochannels

Takashi Kyotani,\* Takayuki Nagai, Sanjuro Inoue, and Akira Tomita

*Institute for Chemical Reaction Science, Tohoku University, Katahira, Sendai 980-77, Japan*

*Received August 12, 1996. Revised Manuscript Received November 20, 1996*<sup>®</sup>

An attempt was made to prepare porous carbon by using the channels of Y zeolite as a template. Poly(acrylonitrile) and poly(furfuryl alcohol) were carbonized in the zeolite channels and the resultant carbon/zeolite complexes were subjected to acid treatment in order to extract carbon from the zeolite framework. In addition, pyrolytic carbon deposition in the channels was carried out by exposing the zeolite to propylene at high temperature, and then the carbon was liberated in the same manner as above. The morphology and structure of the carbon prepared in the channels were characterized, and the results were discussed in relation to the morphology and structure of the original zeolite template. It was found that the microscopic morphology of the resultant carbons reflects that of the corresponding zeolites. All of these carbons are highly porous, and some of the CVD carbons have BET surface areas as high as  $>2000 \text{ m}^2/\text{g}$ .

## Introduction

We have developed a template carbonization technique for synthesizing novel carbon materials. This technique utilizes the inorganic substances whose openings or pores are controlled at nanometer level. Our first attempt was to prepare thin graphite films by the carbonization of organic polymers in the two-dimensional opening between the lamellae of a layered clay such as montmorillonite and taeniolite.<sup>1–5</sup> Recently, we applied this technique to the preparation of one-dimensional carbon such as carbon tubes by using an anodic aluminum oxide film as one-dimensional template<sup>6,7</sup> and obtained uniform hollow nanotubes with open ends.

Zeolites have three-dimensional channels, and their diameter and shape are strictly controlled by the framework topology. Because of the presence of such channels, zeolites have been used as molecular-sieve adsorbents or catalysts. In addition, the well-defined nanospace in a zeolite has been utilized for the synthesis of novel materials. If such a nanospace in a zeolite is packed with carbon and then the carbon is extracted from the zeolite framework, one can expect the formation of a porous carbon whose structure reflects the porosity of the original zeolite template. On the basis of this concept, we made a preliminary attempt to carbonize poly(furfuryl alcohol) in zeolite channels and found the formation of porous carbon.<sup>8</sup> There were a few other reports on carbon formation in zeolite channels. Bein et al. pyrolyzed poly(acrylonitrile) in the channels of Y zeolite and mordenite and then liberated

the resultant carbon from the zeolites using HF solution.<sup>9</sup> Since the carbon obtained thereby showed much lower electronic conductivity than the carbon from bulk poly(acrylonitrile), they concluded that the spatial limitation in the zeolite channels prevents the formation of graphitized structure with high conductivity. Cordero et al. prepared the carbon/zeolite complex with pyrolytic carbon deposition from propylene over zeolite powder as cracking catalyst, followed by dissolving the zeolite with HF and HCl treatment to leave only carbon.<sup>10</sup> Their main purpose was to observe the high-temperature oxidation behavior of the resultant carbon, in comparison with that of pyrolytic carbon-deposited carbon–carbon composites in the same conditions. Very recently, they discussed the oxidation behavior of the carbon extracted from zeolite in relation to its structure.<sup>11</sup> Thus, except for our previous attempt,<sup>8</sup> no one has intentionally utilized zeolite as a template in order to prepare porous carbon. Apart from zeolite, several attempts were made to prepare porous carbon by the template method using silica gel,<sup>12–14</sup> porous glass,<sup>12,13</sup> and sintered sodium chloride.<sup>15</sup> None of these templates, however, has such regular channels as a zeolite has.

Combined with the previous results, we report here our attempt to prepare a new type of porous carbon by using the channels of the Y zeolite as a template. The morphology and structure of the carbon prepared in the channels were characterized by several means. We have paid special attention to how the morphology and

<sup>®</sup> Abstract published in *Advance ACS Abstracts*, January 1, 1997.

- (1) Kyotani, T.; Sonobe, N.; Tomita, A. *Nature* **1988**, *331*, 331.
- (2) Sonobe, N.; Kyotani, T.; Hishiyama, Y.; Shiraishi, M.; Tomita, A. *J. Phys. Chem.* **1988**, *92*, 7029.
- (3) Sonobe, N.; Kyotani, T.; Tomita, A. *Carbon* **1991**, *29*, 61.
- (4) Kyotani, T.; Yamada, H.; Sonobe, N.; Tomita, A. *Carbon* **1994**, *32*, 627.
- (5) Kyotani, T.; Mori, T.; Tomita, A. *Chem. Mater.* **1994**, *6*, 2138.
- (6) Kyotani, T.; Tsai, L.; Tomita, A. *Chem. Mater.* **1995**, *7*, 1427.
- (7) Kyotani, T.; Tsai, L.; Tomita, A. *Chem. Mater.* **1996**, *8*, 2109.
- (8) Kyotani, T.; Nagai, T.; Tomita, A. *Extended Abstracts of Carbon* **1992**, Essen, 437.
- (9) Enzel, P.; Bein, T. *Chem. Mater.* **1992**, *4*, 819.
- (10) Cordero, T.; Thrower, P. A.; Radovic, L. R. *Carbon* **1992**, *30*, 365.
- (11) Rodríguez-Mirasol, J.; Cordero, T.; Radovic, L. R.; Rodríguez, J. J., in preparation.
- (12) Gilbert, M. T.; Knox, J. H.; Kaur, B. *Chromatographia* **1982**, *16*, 138.
- (13) Knox, J. H.; Kaur, B.; Millward, G. R. *J. Chromatogr.* **1986**, *3*, 352.
- (14) Kamegawa, K.; Yoshida, H. *J. Bull. Chem. Soc. Jpn.* **1990**, *63*, 3683.
- (15) Pekela, R. W.; Hopper, R. W. *J. Mater. Sci.* **1987**, *22*, 1840.

structure of the resultant carbon reflect those of the zeolite.

## Experimental Section

**Zeolite Samples as a Template.** The following three types of Y zeolite were used in this study: USY(12) (H-form,  $\text{SiO}_2/\text{Al}_2\text{O}_3 \geq 12$ , Toso Inc., HSZ-360HUA), NaY(5.5) (Na-form,  $\text{SiO}_2/\text{Al}_2\text{O}_3 = 5.5$ , supplied from Dr. H. Terasaki of Tohoku University) and NaY(5.6) (Na-form,  $\text{SiO}_2/\text{Al}_2\text{O}_3 = 5.6$ , Catalysis Society of Japan, JRC-Z-Y5.6). The first zeolite is an ultrastable one, which can keep its crystal structure even at 900 °C. Though the others are not ultrastable, they can stand at 700 °C. Among the three zeolites, NaY(5.5) has the highest crystallinity.

**Carbonization of Poly(acrylonitrile) and Poly(furfuryl alcohol).** We attempted to carbonize poly(acrylonitrile) (PAN) or poly(furfuryl alcohol) (PFA) in the zeolite channels of NaY(5.5) and NaY(5.6). The introduction and polymerization of acrylonitrile in the channels were carried out in the following way. After the powdery zeolite was dried under vacuum at 150 °C, acrylonitrile vapor at its saturated pressure was allowed to contact with the dried zeolite at room temperature for 1 day. Then the acrylonitrile-zeolite complex was evacuated for 30 min in order to remove acrylonitrile adsorbed on the outer surface of zeolite, followed by  $\gamma$ -ray radiation (total dose, 6 Mrad) to polymerize acrylonitrile.

In the case of furfuryl alcohol, it was introduced into NaY(5.6) in liquid phase. The dry powder of the zeolite was impregnated with furfuryl alcohol under reduced pressure at room temperature. The mixture of furfuryl alcohol and zeolite powder was stirred for more than 5 days, and then it was filtered, followed by washing with mesitylene to remove furfuryl alcohol on the external surface of zeolite powder. The polymerization of furfuryl alcohol in zeolite was carried out by heating the powder under  $\text{N}_2$  flow at 80 °C for 24 h and then at 150 °C for 8 h. The resultant PAN/zeolite and PFA/zeolite complexes were heat-treated at a linear rate of 5 °C/min to 700 °C and held there for 3 h to carbonize the polymers in the zeolite channels. The carbon/zeolite complexes were washed with an excess amount of 46% aqueous HF solution at room temperature and subsequently refluxed in 36% aqueous HCl solution to dissolve the zeolite framework. As a result, carbon was obtained as an insoluble fraction.

**Chemical Vapor Deposition (CVD) over Zeolite.** Only USY(12) was employed for CVD in zeolite channels, because of its high thermal stability. The dried powdery zeolite was placed in a vertical quartz reactor (i.d., 16 mm). The reactor temperature was raised to 800 °C under  $\text{N}_2$  flow, and then propylene gas (2.5% in  $\text{N}_2$ ) was passed through the reactor at a total flow rate of 200  $\text{cm}^3$ (STP)/min. The thermal decomposition of propylene in zeolite results in pyrolytic carbon formation in its channels. After the desired period of time, the reactor was cooled to room temperature. The zeolite framework in the carbon/zeolite complex was dissolved by successive washing with HF and HCl solutions, leaving only carbon as an insoluble fraction in the solution.

Y zeolite has an open pore size of about 0.74 nm, which is large enough for acrylonitrile, furfuryl alcohol and propylene molecules to diffuse.

**Characterization.** The microscopic features of the complexes and the carbons were observed with a scanning electron microscope (SEM, Hitachi, S900) and transmission electron microscopes (TEM, JEOL: JEM-2000EXII, JEM-3010, and JEM-ARM1250). To observe the inside of the sample, several carbon particles were embedded in an epoxy resin and sliced at a thickness of less than 100 nm with an ultramicrotome. Then their TEM observation was performed. The structure change of the complexes with the heat and acid treatments and the crystallinity of the resultant carbons were examined with an X-ray diffractometer (XRD, Shimadzu, XD-D1 with Cu K $\alpha$  radiation) by referring to a silicon standard. The surface area and the pore structure of the samples were investigated with an automatic volumetric sorption analyzer (Quantachrome, Autosorb-1) using  $\text{N}_2$  as adsorbent at -196 °C. The surface area and the micropore volume were, respec-

**Table 1. Amount of Carbon in the Carbon/Zeolite Complexes and the Results of Elemental Analysis for the Carbons after the Acid Washing**

carbon precursor	zeolite	carbon deposition period (h)	carbon content (g/g of zeolite)	elemental analysis for the carbon (wt %)			
				C	H	N	O (diff)
PAN	NaY(5.5)		0.21	69	3	9	19
PAN	NaY(5.6)		0.18	74	3	10	13
PFA	NaY(5.6)		0.17	90	3	0	7
propylene	USY(12)	1	0.11	89	3	0	8
propylene	USY(12)	3	0.23	91	2	0	7
propylene	USY(12)	6	0.42	96	2	0	2
propylene	USY(12)	12	0.55	98	2	0	0

tively, determined from the BET equation and the Dubinin-Radushkevich equation. The mesopore volume was calculated by subtracting the micropore volume from the volume of  $\text{N}_2$  adsorbed at a relative pressure of 0.95.

## Results

**Elemental Analysis.** Table 1 shows the amount of the carbon formed in zeolites. This value was determined from the amount of the combustible part in each carbon/zeolite complex. For all the complexes from PAN and PFA, the amounts of carbon are almost 0.2 g/g of zeolite. The carbon content in the complexes with pyrolytic carbon increases with carbon deposition period. The last part in Table 1 summarizes the results of the elemental analysis for the carbon samples after the acid washing. For all the samples, their ash content (not shown here) was found to be less than 0.5%. Some of the samples include significant amount of oxygen, even though their precursors do not have oxygen, like PAN or propylene. Most of such oxygen was probably incorporated into carbon during the washing process, because the carbon/zeolite complexes from PAN and propylene have almost no oxygen.

**SEM Observation.** Figure 1 shows the SEM photographs of the three types of zeolites, and their corresponding carbon/zeolite complexes and carbons. The photographs of the zeolites (the left side of Figure 1) confirm that the crystallinity of NaY(5.5) is highest among the three zeolite samples. Some of the particles seem to be a single crystal. The next highest one is USY(12), whose particle size is somewhat smaller than that of NaY(5.5). In both the zeolites, clear crystal faces were observed on many particles. The particles of NaY(5.6) have a larger diameter (0.8–1.2  $\mu\text{m}$ ), and they look comprised of several small zeolite crystals. There is almost no difference in morphology between the zeolites and the corresponding complexes (the middle of Figure 1).

The right side of Figure 1 shows the SEM photographs of the carbon samples. The most remarkable feature of the appearance of these carbons is a strong resemblance to that of the corresponding template. For instance, the PAN carbon particles from NaY(5.6) appear to consist of several small parts. This feature is exactly the same as in the corresponding template, NaY(5.6). It was also the case with the PFA carbon from NaY(5.6) (not shown here). Despite such resemblance, the particle size of the carbons from PAN or PFA is always smaller than that of the corresponding zeolites. In the case of the CVD carbon, the smooth surface of the carbon particles looks like a result of the inheritance of the crystal face of the USY(12) particles. The particle size of these carbons is almost the same as that of USY(12).

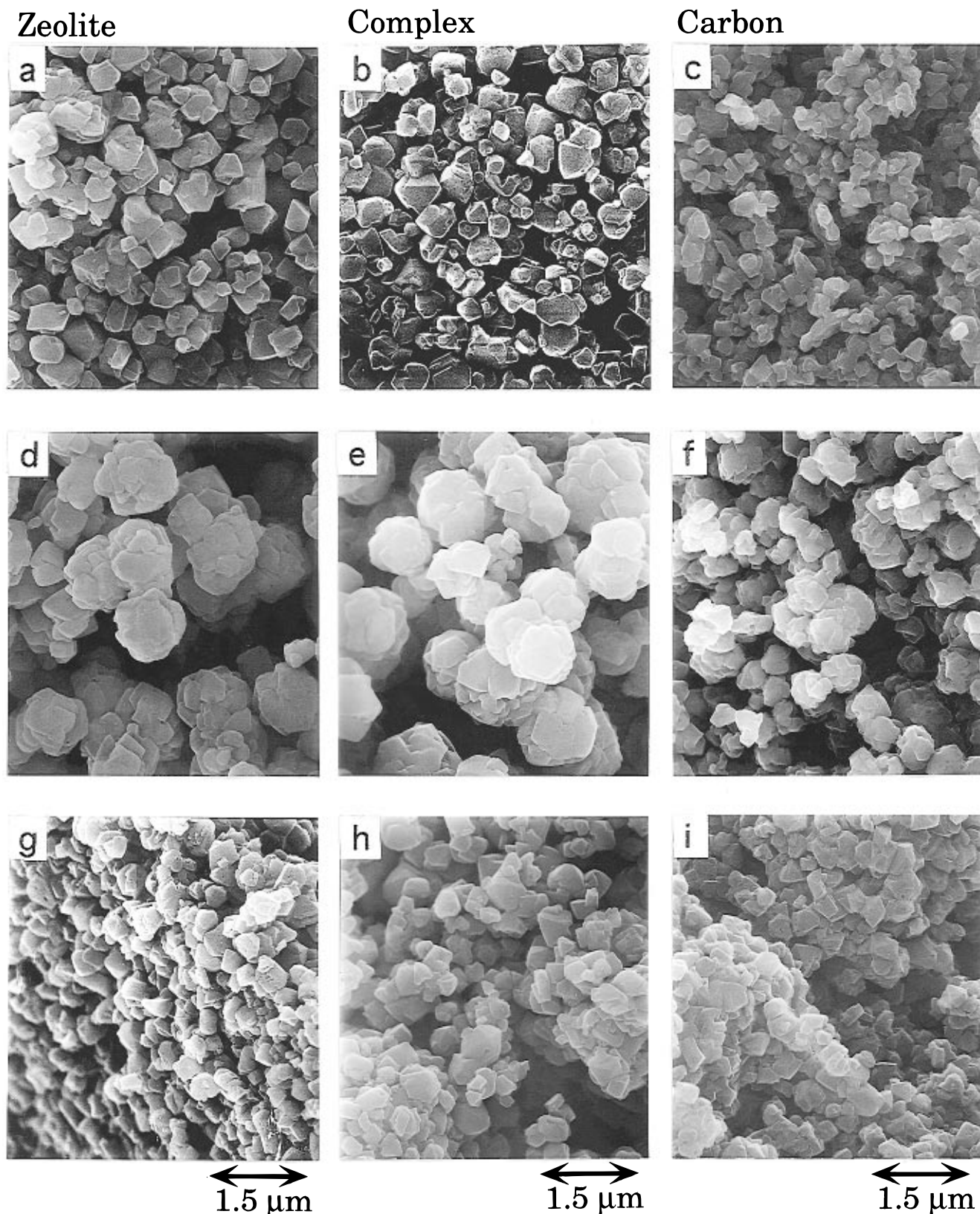


**Figure 1.** SEM photographs of the zeolites (the left-hand side), the carbon/zeolite complexes (the middle) and the carbons (the right): (a) NaY(5.5); (b) PAN carbon/NaY(5.5); (c) PAN carbon from NaY(5.5); (d) NaY(5.6); (e) PAN carbon/NaY(5.6); (f) PAN carbon from NaY(5.6); (g) USY(12); (h) CVD carbon/USY(12) (CVD period, 3 h); (i) CVD carbon from the sample (h).

**TEM Observation.** Figure 2 presents the TEM photographs of the carbons prepared from the polymers. The bright-field image of the PAN carbon from NaY(5.5) (Figure 2a) displays a particle with a size of about  $0.3\ \mu\text{m}$ , which corresponds to the carbon particles as observed in the SEM photograph (Figure 1c). The image is so dark that we cannot see its detailed

structure. The TEM image of the sliced sample of the PAN carbon from NaY(5.5) is shown in Figure 2b. The bright and gray parts in this image, respectively, correspond to the cross sections of epoxy resin and carbon particles embedded in the resin. Almost no voids are observed in the carbon particles. In the bright-field images of the PAN and PFA carbons from NaY(5.6)

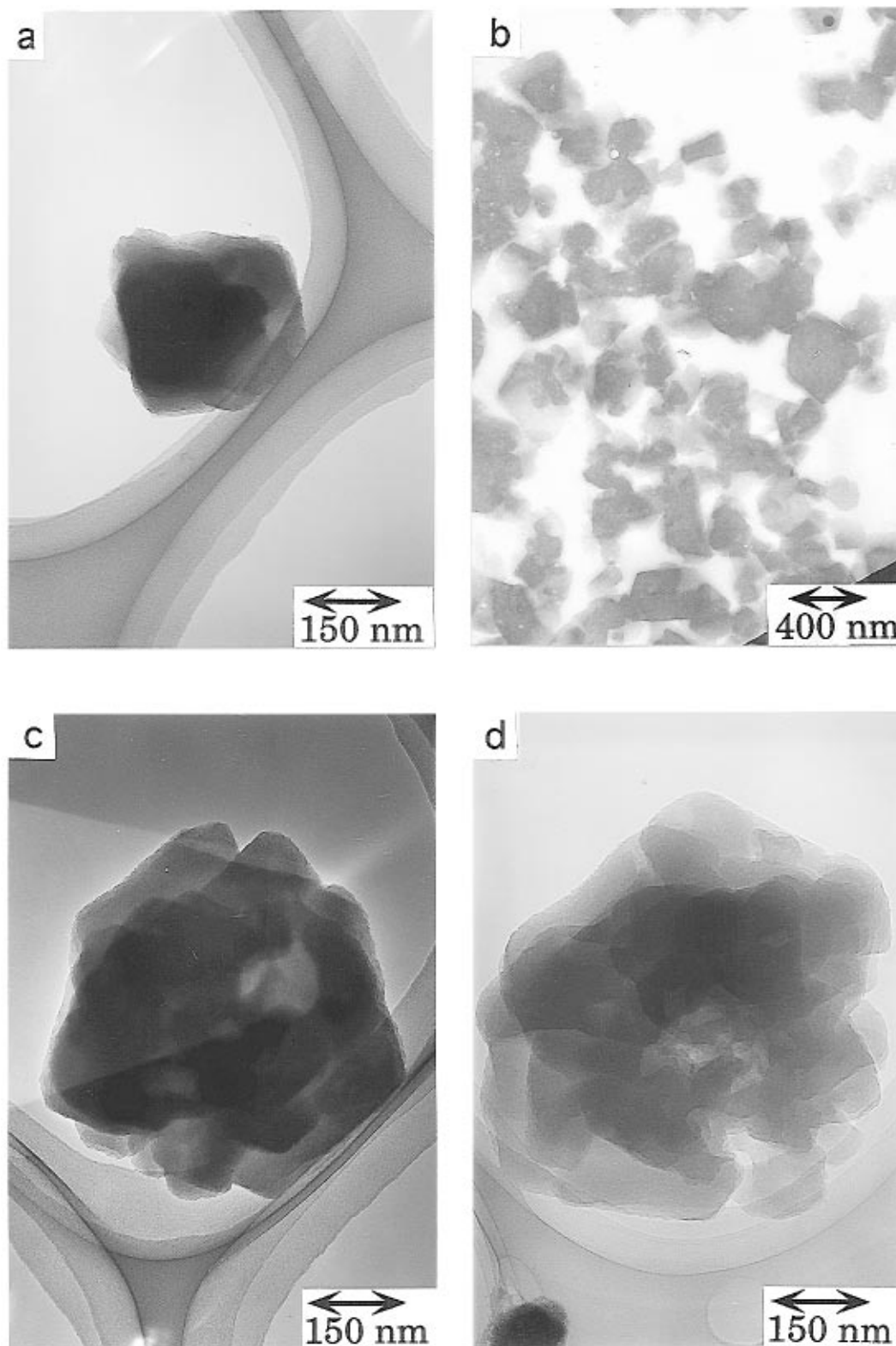


**Figure 2.** TEM images of the polymer carbons prepared in the zeolite channels (a microscope grid is seen under the samples): (a, b) PAN carbon from NaY(5.5), ((b) is the TEM image of its sliced sample); (c) PAN carbon from NaY(5.6); (d) PFA carbon from NaY(5.6).

(Figure 2c,d), dense and sparse portions are observed and these images reflect the morphology which is seen in the SEM photograph (Figure 1f).

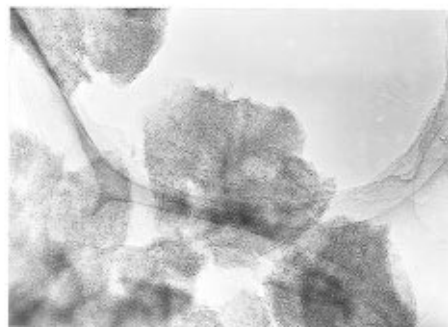
Figure 3 shows the TEM photographs of the CVD carbons with different carbon deposition periods. The particles in the top TEM photograph correspond to the carbon particles in Figure 1i. It should be noted that the carbon particles with the 12 h deposition have thin and denser carbon envelope on each particle, but the

other two images do not show such a layer. Since the layer was observed only as the envelope of particles, it must be ascribed to the carbon deposited on the external surface of the zeolite particles.

**XRD Analysis.** The XRD patterns for the carbon/zeolite complexes exhibited many sharp peaks, all of which can be assigned to Y zeolite. This suggests that the framework of the zeolite was kept intact even after the heat treatment. The XRD patterns for the PAN and

Carbon  
deposition  
period:

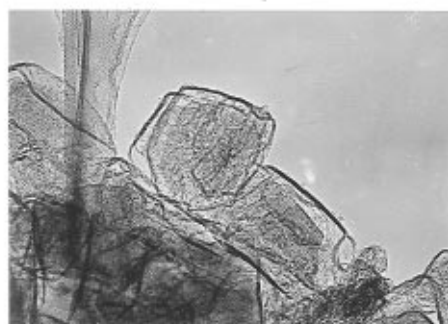
3 h



6 h



12 h



150 nm

**Figure 3.** TEM images of the CVD carbons prepared in the USY(12) zeolite under different carbon deposition periods (a microscope grid is seen under the samples).

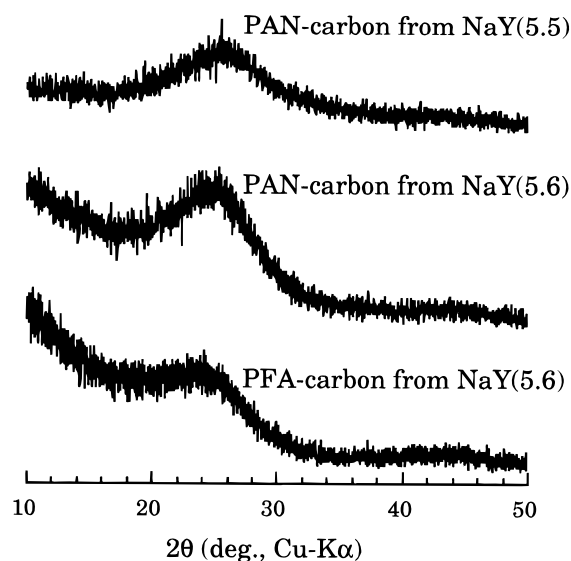


**Figure 4.** XRD patterns for the polymer carbons prepared in NaY zeolite.

PFA carbons are given in Figure 4, where a broad (002) diffraction peak is observed, but no other peak appears. The structural parameters such as the interplanar spacing ( $d_{002}$ ) and the average crystallite size ( $L_c$ ) were, respectively, determined from the position and the half-

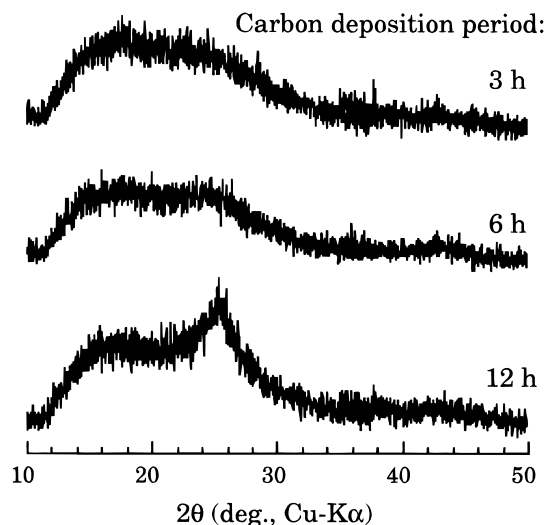


**Figure 5.** XRD patterns for the CVD carbons prepared in the USY(12) zeolite under different carbon deposition periods.

width of each (002) peak. The values of  $d_{002}$  were 0.35, 0.35, and 0.36 nm for the PAN carbons from NaY(5.5) and NaY(5.6) and the PFA carbon from NaY(5.6), respectively. These values are much larger than that of ideal graphite ( $d_{002} = 0.3354$  nm), indicating low crystallinity of these carbons. The  $L_c$  values for the polymer carbons ranged from 1.4 to 1.5 nm.

Figure 5 illustrated the XRD patterns of the CVD carbons with different carbon deposition periods. The pattern depends on the carbon deposition period. In the case of the sample with the 3 h deposition, we can observe no peak at around  $25^\circ$ . After a 6 h deposition, the (002) peak is still unclear. The 12 h carbon deposition, however, gives a relatively sharp (002) peak with  $d_{002}$  of 0.351 nm and  $L_c$  of 2.8 nm.

**N<sub>2</sub> Adsorption.** Figure 6 shows the N<sub>2</sub> isotherms on the zeolites and carbon/zeolite complexes at  $-196^\circ\text{C}$ . As well as the zeolite samples, the complexes show a rapid increase in their adsorption isotherms at a very low relative pressure. Even for the complex prepared by the 6 h carbon deposition, there is a small increase in adsorption at a low pressure (Figure 6i). This finding indicates that these complexes still have micropores. In the cases of the complex with the 12 h deposition (not shown here), its isotherm did not show such a rapid increase. This may be due to the pore blockage on the external surface of the zeolite particles. We will discuss more details of this later.

The N<sub>2</sub> isotherms on the carbon samples are illustrated in Figure 7, where all the isotherms suggest the presence of micropores in these carbons. This figure clearly indicates that N<sub>2</sub> adsorbs on the CVD carbons much more than on the PAN and PFA carbons. From these isotherms, we determined their BET surface area, micropore and mesopore volumes, which are summarized in Tables 2 and 3. Table 3 also includes the data of the CVD carbons prepared under the other deposition conditions. The values of the surface area and the pore volumes for the CVD carbons are significantly larger than those for the polymer carbons. Some of the CVD carbons have BET surface areas of more

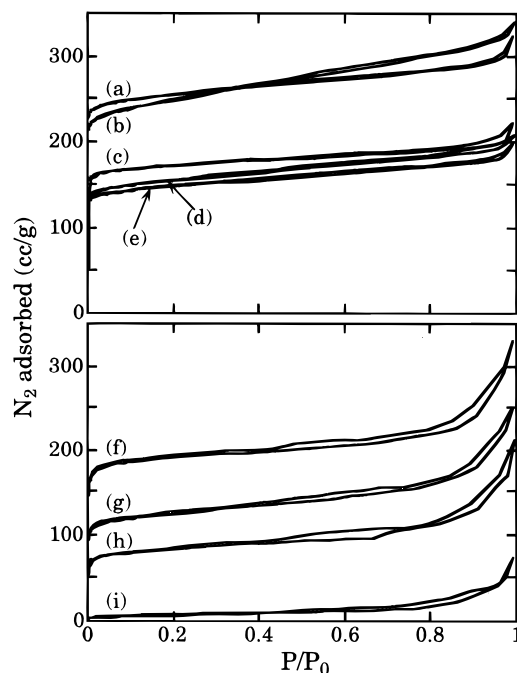


**Figure 6.**  $N_2$  isotherms for the zeolites and the carbon/zeolite complexes: (a) NaY(5.5); (b) NaY(5.6); (c) PAN carbon/NaY(5.5); (d) PAN carbon/NaY(5.6); (e) PFA carbon/NaY(5.6); (f) USY(12); (g), (h), and (i) CVD carbon/USY(12) complexes prepared under carbon deposition periods of 1, 3, and 6 h, respectively. For each isotherm, the upper and lower curves correspond to the desorption and adsorption isotherms, respectively.

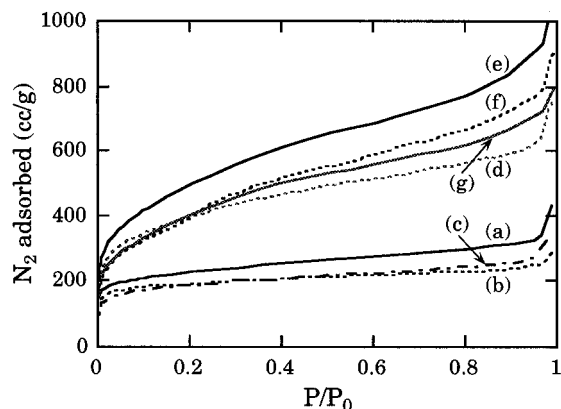


**Figure 7.** Adsorption isotherms for  $N_2$  on the carbons prepared in the zeolite channels: (a) PAN carbon from NaY(5.5); (b) PAN carbon from NaY(5.6); (c) PFA carbon from NaY(5.6); (d), (e), (f), and (g) CVD carbons from USY(12) under carbon deposition periods of 1, 3, 6, and 12 h, respectively.

**Table 2. Pore Structure of the Polymer Carbons Prepared in the Zeolite Channels**

sample	BET surface area ( $m^2/g$ )	micropore vol ( $cm^3/g$ )	mesopore vol ( $cm^3/g$ )
PAN carbon from NaY(5.5)	700	0.31	0.20
NaY(5.6)	580	0.28	0.10
PFA carbon from NaY(5.6)	590	0.28	0.15

than  $2000 m^2/g$ . The micropore volume of each polymer carbon is always larger than its mesopore volume, while the micro- and mesopores have comparable volume for most of the CVD carbons.

We can evaluate from Table 3 the optimum deposition conditions for obtaining carbon with high surface area. A lower reaction temperature ( $700^\circ C$ ) or lower propyl-

**Table 3. Effect of Carbon Deposition Conditions on Pore Structure of the CVD Carbons Prepared in the Zeolite Channels**

deposition temp ( $^\circ C$ )	propylene concn (% in $N_2$ )	deposition period (h)	BET surface area ( $m^2/g$ )	micropore vol ( $cm^3/g$ )	mesopore vol ( $cm^3/g$ )
800	2.5	1	1320	0.54	0.42
800	2.5	3	1720	0.69	0.71
800	2.5	6	1510	0.55	0.64
800	2.5	12	1430	0.57	0.52
800	1.3	12	2060	0.82	0.75
800	1.3	15	2200	0.88	0.83
800	1.3	18	1790	0.72	0.62
700	2.5	12	1660	0.66	0.79
700	2.5	18	2260	1.11	0.76

ene concentration (1.3%) favors the production of high surface area carbon, that is, high surface area can be obtained at a low carbon deposition rate. Too long carbon deposition, however, reduces its surface area.

## Discussion

Table 1 indicates that most of the carbon/zeolite complexes include about 0.2 g of carbon/g of zeolite. If these large amounts of carbons are present mainly on the external surface of the zeolite crystals, we should have observed significant difference in morphology between the pure zeolite crystals and the corresponding complexes. Moreover, their TEM images should have shown a void inside each carbon particles, because the removal of zeolite framework mainly leaves carbon envelope over the particles. The SEM and TEM observations, however, did not give such microscopic features; we observed no remarkable carbon deposit on the external surface of the zeolite crystals and no clear void in each particle. This is more obvious with the TEM image of the sliced carbon samples (Figure 2b), where we observed no void inside each particle. This is a direct evidence of the presence of carbon in the nanochannels of the zeolites.

According to the Dubinin–Radushkevich plot, the micropore volume of the zeolites was calculated to be about  $0.30 cm^3/g$  for USY(12),  $0.38$  for NaY(5.5), and  $0.36$  for NaY(5.6). If the carbon is packed only in the micropores of the zeolite, the maximum amount of packed carbon can be calculated by assuming that the carbon in the nanochannels has the same density as that of graphite ( $2.26 g/cm^3$ ). These values were 0.68, 0.86, and  $0.81 g$  for USY(12), NaY(5.5), and NaY(5.6), respectively. The actual amounts of carbon are always less than the theoretical one (see Table 1). Furthermore, the isotherms of the complexes suggest that some micropores are still present in the complexes. Hence, in every case the carbon packing does not reach complete filling in the zeolite channels. In the case of the polymer carbon complexes, such incomplete filling would be mainly due to the weight loss of the polymer during its carbonization in the channels.

The CVD carbon with a 12 h deposition has dense carbon layers (Figure 3). Such carbon deposition would result in the complete pore blockage of zeolite, which explains the absence of micropores in the corresponding carbon/zeolite complex.

Despite the fact that the polymer carbons gave the carbon (002) diffraction peak, the XRD patterns for the corresponding carbon/zeolite complexes did not exhibit this carbon peak. One of the possible reasons for this is that the amount of the polymer carbon in the



complexes was not large enough to give a (002) peak. To clarify this point, we made an XRD analysis for a physical mixture of NaY(5.6) and the PAN carbon isolated from a NaY(5.6) matrix. The amount of carbon in this mixture was adjusted to be equal to that in the PAN carbon/NaY(5.6) complex. The resultant XRD pattern of this mixture showed a very weak but detectable (002) diffraction. The absence of the (002) peak in the complexes must be, therefore, ascribed not to the low carbon content but to another reason. The most probable explanation is that a carbon stacking structure cannot be developed in such a small space as a zeolite channel. For the polymer carbons, the appearance of (002) peak after the acid washing suggests that carbon layers were stacked together upon the removal of zeolite framework. The  $L_c$  values for the polymer carbons (1.4–1.5 nm) are larger than the size of a supercage (1.2 nm) of Y zeolite. This fact also suggests that carbon layers were stacked after they were extracted from the zeolite. From the SEM photographs of these carbons, we observed the size of the carbon particles to be always smaller than that of the corresponding carbon/zeolite complex particles, despite little morphological change. The carbon layer stacking during the washing might be related to this shrinkage in size.

In contrast to the carbons from the polymers, the CVD carbon with the 3 h deposition did not give any (002) peak even after isolation, indicating no stacking structure and extremely poor crystallinity of this carbon. A similar XRD pattern was reported for the activated carbons with high surface area, which were activated by KOH.<sup>16</sup> On the other hand, a sharp (002) peak was observed for the carbon with the 12 h deposition. The possible origin for this sharp peak would be the dense carbon layers on the outer surface of the carbon particles as observed in Figure 3.

The  $N_2$  adsorption results revealed that all the carbons prepared in the zeolite channels are highly porous. The porosity of these carbons originates from the porous structure of the Y zeolite. The zeolite framework in the carbon/zeolite complex would convert to the pore of the resultant carbon after the acid washing. The CVD carbons have a higher surface area, and some of them are more than 2000 m<sup>2</sup>/g. The lower surface area and pore volumes of the polymer carbons can be partially attributed to the stacking of carbon layers during the acid washing, because such stacking

may cause the disappearance of some pores and/or the reduction in pore size.

To the best of our knowledge, this study is the first report on preparing porous carbon with a surface area of more than 2000 m<sup>2</sup>/g without any conventional activation using gas or chemicals. Furthermore, our method makes it possible to prepare high surface area carbon without carbon consumption, while any activation process consumes carbon to a substantial extent. For example, activated carbons prepared by chemical treatment with KOH have a high BET surface area of 2500–4500 m<sup>2</sup>/g,<sup>16–18</sup> but such a high surface area as 4500 m<sup>2</sup>/g was obtained with a carbon loss of as much as 75%.<sup>19</sup> Most of the pores in this type of activated carbon are dominated by micropores.<sup>18,19</sup> The porosity of the CVD carbons prepared by the present method, however, consists of not only micropores but also a considerable amount of mesopores.

### Conclusions

For the carbon/zeolite complexes, we confirmed the presence of carbon in the nanochannels of Y zeolite. The carbon packing in the channels was, however, not complete, and there are still some space unoccupied by carbon. The carbon in the channels did not have any regular stacking structure as carbon usually has. This is due to the spatial limitation of the zeolite channels.

It was found that the microscopic morphology of each zeolite exactly reflects that of the corresponding carbon. All of these carbons are highly porous. We can conclude that the channel structure of Y zeolite endowed the resultant carbon with its porosity. The CVD carbons have higher surface area and larger pore volume than those of the polymer carbons. The BET surface area of the former carbons could reach more than 2000 m<sup>2</sup>/g, when their deposition conditions were optimized. This is the first example of preparing porous carbon with such a high surface area without any activation process. Unlike the high surface area carbon prepared by chemical activation with KOH, mesopores, as well as micropores, are well developed in the CVD carbons.

**Acknowledgment.** We thank the High Voltage Electron Microscope Laboratory of Tohoku University and Dr. N. Sonobe of Kureha Chemical Industry Co., Ltd., for microscopical analysis. We are indebted to Dr. H. Terasaki of Tohoku University for the preparation of zeolite sample. Thanks are also due to Dr. J. Rodríguez-Mirasol of University of Málaga for his helpful discussion. This study was partly supported by Special Coordination Funds for Promising Science and Technology from Science and Technology Agency, Japan.

CM960430H

(16) Shiraishi, M.; Yoshizawa, N.; Ohkawa, K.; Maeda, T. *Tanso* **1992**, 155, 295.

(17) Marsh, H.; Crawford, D.; O'Grady, T. M.; Wennerberg, A. *Carbon* **1982**, 20, 419.

(18) Matsumura, Y. *Chem. Chem. Ind.* **1990**, 43, 358.

(19) Maeda, T. In *Kyuchaku Gijyutsu Handbook*; Shimizu, H., Ed.; NTS: Tokyo, 1993; Chapter II-1-3; p 154.